

Natural Time Analysis: Results Related to Two Earthquakes in Greece during 2019 [†]

Nicholas V. Sarlis ^{1,2}, Efthimios S. Skordas ^{1,2} and Panayiotis A. Varotsos ^{1,2,*}

¹ Section of Solid State Physics, Department of Physics, National and Kapodistrian University of Athens, Panepistimiopolis, 157 84 Zografos, Athens, Greece; nsarlis@phys.uoa.gr (N.V.S.); eskordas@phys.uoa.gr (E.S.S.)

² Solid Earth Physics Institute, Department of Physics, National and Kapodistrian University of Athens, Panepistimiopolis, 157 84 Zografos, Athens, Greece

* Correspondence: pvaro@otenet.gr; Tel.: +30-2107276737

[†] Presented at the 2nd International Electronic Conference on Geosciences, 8–15 June 2019; Available online: <https://iecg2019.sciforum.net/>.

Published: 4 June 2019

Abstract: The following two earthquakes occurred in Greece during 2019: First, a M_w 5.4 earthquake close to Preveza city in Western Greece on 5 February and a M_w 5.3 earthquake 50 km East of Patras on 30 March. Here, we present the natural time analysis of the Seismic Electric Signals (SES) activities that have been recorded before these two earthquakes. In addition, we explain how the occurrence times of these two earthquakes can be identified by analyzing in natural time the seismicity subsequent to the SES activities.

Keywords: seismicity; earthquake prediction; natural time; seismic electric signals; Greece

1. Introduction

According to the United States Geological Survey (USGS) [1], a strong earthquake (EQ) of moment magnitude M_w 6.8 occurred on 25 October 2018 22:55 UTC at an epicentral distance around 133 km SW of the city of Patras, Western Greece (see Figure 1). It was preceded by an anomalous geoelectric signal that was recorded on 2 October 2018 at a measuring station 70km away from the epicenter [2]. Upon analyzing this signal in natural time, it was found [2] that it conforms to the conditions suggested (e.g., see [3–5]) for its clarification as precursory Seismic Electric Signal (SES) activity [4,6,7]. Notably, the observed lead time of 23 days lies within the range of values that has been very recently identified [8] as being statistically significant for the precursory variations of the electric field of the Earth. Moreover, the analysis in natural time of the seismicity subsequent to the SES activity in the area revealed [2] that critical conditions were obeyed early in the morning of 18 October 2018, i.e., almost a week before the strong earthquake occurrence, in agreement with earlier findings [4]. The application [2] of the recent method of nowcasting earthquakes [9–13], which is based on natural time, has revealed that an earthquake potential score of around 80% was observed just before the occurrence of this M_w 6.8 earthquake. Here, we focus on the recording [14] of additional SES activities after the occurrence of the latter earthquake in the beginning of January 2019 (see below) that preceded the following two earthquakes in Greece during 2019: First, a M_w 5.4 earthquake [15] close to Preveza city in Western Greece on 5 February 2019 and a M_w 5.3 earthquake [16] on 30 March 2019 a few tens of km East of Patras SES measuring station (labeled PAT in Figure 1).

2. Results

Two SES activities were recorded [14] by the VAN telemetric network [3] operating in real time in Greece on 3 January 2019 and 9 January 2019 at the measuring stations PAT and PIR, respectively (see Figure 1).

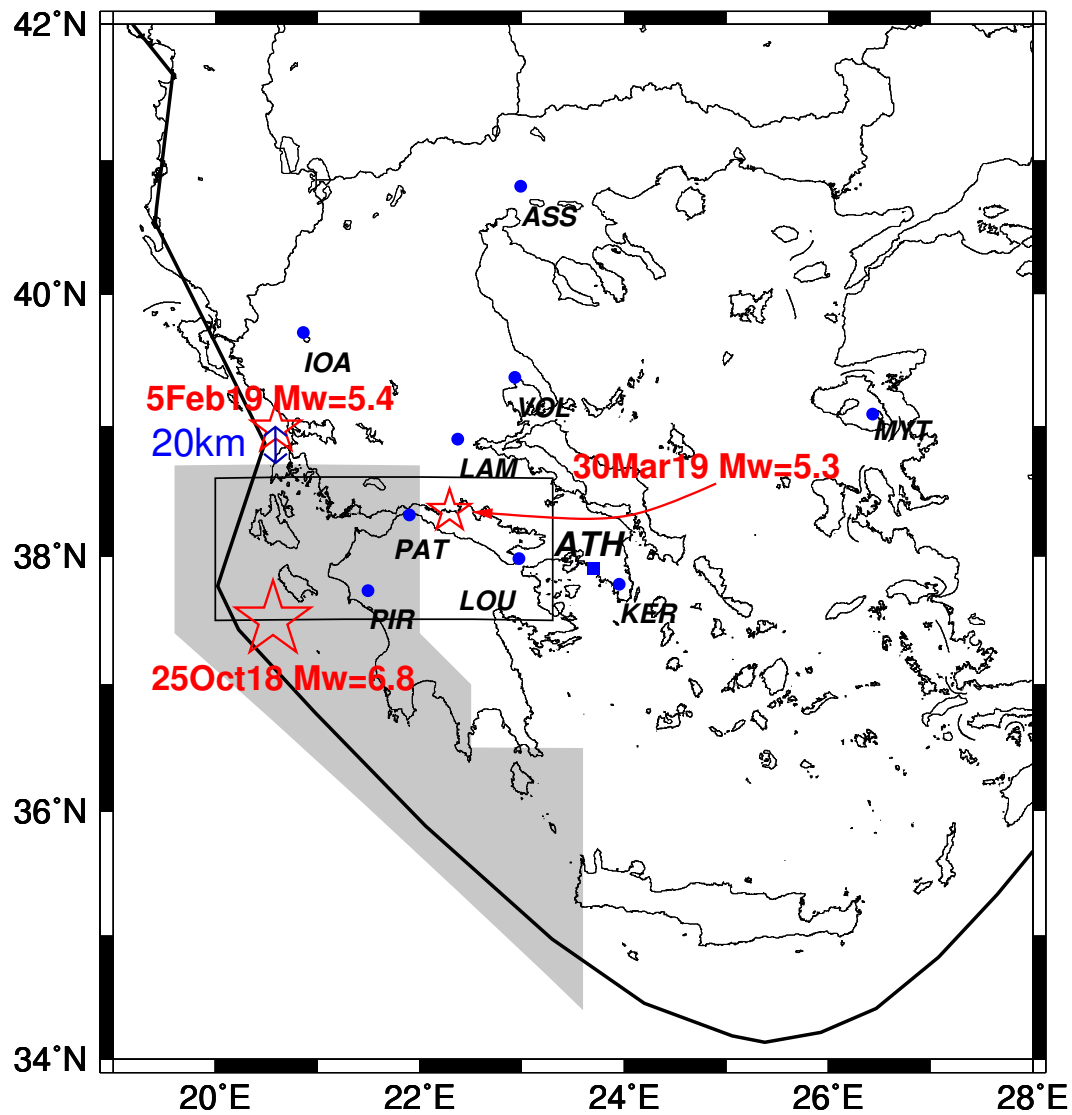


Figure 1. Map of the area $N_{34}^{42}E_{19}^{28}$ in which the locations of the SES measuring stations of the VAN telemetric network [3] operating in Greece are shown by the blue circles. The blue square corresponds to the central station operating at Glyfada, Athens (ATH), where the data are collected. The thick black line depicts the Hellenic arc [17] while the gray shaded area and the black rectangle the selectivity map of Pargos (PIR) measuring station (see Figure 1 in [2]) and Patras (PAT) measuring station (see the rectangle with solid lines in Figure 8 in [18]), respectively. After the recording of the SES activities on 3 January 2019 at PAT and on 9 January 2019 at PIR, the areas corresponding to the selectivity maps of these two measuring stations have been reported in [14] as probable to suffer a strong EQ. The red stars correspond to the epicenters of the M_w 6.8 EQ on 25 October 2018, the $M_w = 5.4$ EQ on 5 February 2019, and the $M_w = 5.3$ EQ on 30 March 2019.

According to the VAN method of short-term earthquake prediction [3,4,6,7,19–21], the electric signals that are emitted from the future focal area as the stress increases prior to the EQ due to the collective (re)orientation (cf. such a cooperativity is a hallmark showing that the region enters the critical stage) [22] of the pre-existing electric dipoles [23] in the ionic constituents of the rocks, e.g., see Figure 1

in [24], follow [7], conductive paths in the solid Earth crust and become detectable at certain (SES sensitive) sites on the Earth's surface giving rise to the so-called selectivity phenomenon [7,17,25–31]. This means that an SES measuring station is capable of recording SESs emitted from certain EQ prone areas. After long experimentation (cf. SES research in Greece started in the 1980s, e.g., see [32,33]) for each measuring station, one may construct a selectivity map of this station by considering the EQs that have been preceded by SES recorded in the station as well as by using geological and geophysical data (since faults are usually highly more conductive than their surroundings, they constitute conductive paths, e.g., see [25]). The gray shaded area in Figure 1 depicts the selectivity map of the PIR measuring station as reported in [2] while the black rectangle in the same figure corresponds to the selectivity map of the PAT measuring station [14,18].

The SES activity recorded on 3 January 2019 at PAT station can be seen in Figure 5 in [14]. The analysis in natural time has led [14] to values of κ_1 , S and S_- which are compatible with those observed for SES (see Section 4.1). After applying the methodology suggested in [34] for the analysis of the SES activity recorded on 3 January 2019 at PAT we obtain $\kappa_1 = 0.075(22)$, $S = 0.071(22)$, and $S_- = 0.075(30)$. More or less similar results are found for the SES recorded on 9 January 2019 at PIR.

After these observations and in order to estimate the occurrence time of the impending EQs, we started to analyze in natural time the seismic activity occurring after the SES within the respective selectivity maps of each measuring station, i.e., the gray shaded area of Figure 1 for PIR and the one shown by the black rectangle in Figure 1 for PAT. We observed (see Figure 7 in [35]) that when analyzing the seismicity within the PIR selectivity map, the criticality condition $\kappa_1 = 0.070$ has been fulfilled upon the occurrence of a $ML(ATH) = 3.5$ EQ at 12:50 UTC on 29 January 2019 at 37.69° N 20.61° E exhibiting magnitude threshold invariance. Here, $ML(ATH)$ stands for the local magnitude reported by the Institute of Geodynamics of the National Observatory of Athens. A week later, i.e., at 02:26 UTC on 5 February 2019, an $M_w 5.4$ EQ occurred with an epicenter at 38.98° N 20.59° E lying very close to the NorthWestern edge of the PIR selectivity map, see Figure 1. The corresponding natural time analysis of the seismicity within the PAT selectivity map (see the black rectangle in Figure 1) after the SES activity on 3 January 2019 has shown that upon the occurrence of the $ML(ATH) = 3.2$ EQ at 06:53 UTC on 23 March 2019 at 37.69° N 20.61° E the condition $\kappa_1 = 0.070$ has been met for various magnitude thresholds (see Figure 9 of [35]). Interestingly, almost a week later the $M_w = 5.3$ EQ of Figure 1 occurred at 10:46 UTC on 30 March 2019 with an epicenter at 38.35° N 22.29° E lying inside the PAT selectivity map at a distance around 30km from the PAT measuring station.

3. Discussion

It is notable that the occurrence of the two EQs under study took place almost a week after the criticality condition $\kappa_1 = 0.070$ has been met for various magnitude thresholds. This compares favorably with the time window of a few days up to one week already found from various SES activities in Greece, Japan and United States [2,4,18,36–39].

4. Materials and Methods

4.1. Natural Time Analysis (NTA)

In a time series consisting of N individual events (e.g., electric pulses or EQs), the natural time [4,40–42] associated with the k -th event is given by $\chi_k = k/N$. In NTA [4,40–42], the pair (χ_k, Q_k) is studied, where Q_k is proportional to the energy emitted during the k -th event. For example in the case of SES, Q_k is proportional to the duration of each SES pulse [40,41], while for EQs it may be considered proportional to the seismic moment [40,42,43]. How the time series coming from a variety of complex systems are read in natural time can be seen in Figure 1 of [5].

The pair (χ_k, Q_k) is studied by considering the normalized energy for the k -th event $p_k = Q_k / \sum_{n=1}^N Q_n$, where p_k can be also considered as a probability distribution [5,44]. In view of the latter, the function [4,40–42,44]

$$\Pi(\omega) = \left| \sum_{k=1}^N p_k \exp\left(i\omega \frac{k}{N}\right) \right|^2 \tag{1}$$

provides information about the probability distribution p_k when $\omega \rightarrow 0$. Expanding Equation(1) around $\omega = 0$, we obtain that $\Pi(\omega) = 1 - \kappa_1 \omega^2 + \dots$, where κ_1 stands for the variance of natural time

$$\kappa_1 \equiv \sum_{k=1}^N \chi_k^2 p_k - \left(\sum_{k=1}^N \chi_k p_k \right)^2, \tag{2}$$

with respect to the distribution p_k . When Q_k are independent and identically distributed random variables, we have that $p_k \rightarrow 1/N$. This is the case of the so-called [4,45,46] ‘uniform’ distribution leading to a value of κ_1 equal to $\kappa_u = 1/12 \approx 0.083$. For critical systems, Varotsos et al. [47] have shown that

$$\kappa_1 \approx 0.07 \tag{3}$$

for a variety of systems approaching criticality. Thus, κ_1 reaches the value of 0.070 for a critical system or 0.083 for a system exhibiting stationary or quasi-periodic behavior [5].

Apart from κ_1 , another useful quantity in NTA [4,5] is the entropy S given by [40,46,48]

$$S = \langle \chi \ln \chi \rangle - \langle \chi \rangle \ln \langle \chi \rangle, \tag{4}$$

where the brackets $\langle \dots \rangle$ ($\equiv \sum_{k=1}^N \dots p_k$) denote averages with respect to the distribution p_k . The entropy S is a dynamic entropy that exhibits [49] positivity, concavity and Lesche [50,51] experimental stability. When Q_k are independent and identically distributed random variables, S reaches [48] the value $S_u \equiv \frac{\ln 2}{2} - \frac{1}{4} \approx 0.0966$ that corresponds to the aforementioned ‘uniform’ distribution. For SES, it has been experimentally observed [4,49] that $S_{\text{SES}} \lesssim S_u$. Upon reversing the time arrow and hence applying the time reversal operator \mathcal{T} to p_k , i.e., $\mathcal{T} p_k = p_{N-k+1}$, the value of S changes to a value S_- . Again, it has been experimentally observed [4,49] that for SES activities: $S_- \lesssim S_u$.

5. Conclusions

The two strongest earthquakes that occurred in Greece since 1 January 2019, i.e., the Mw5.4 earthquake close to Preveza city in Western Greece on 5 February and the Mw5.3 earthquake 50km East of Patras on 30 March, were preceded by Seismic Electric Signals (SES) activities that were identified as such before the earthquakes [14].

The occurrence times of these two earthquakes can be approached by analyzing in natural time the seismicity subsequent to the SES activities within the selectivity maps of the corresponding VAN stations that recorded the SES activities.

Author Contributions: Conceptualization, N.V.S., E.S.S. and P.A.V.; Methodology, N.V.S., E.S.S. and P.A.V.; Software, N.V.S. and E.S.S.; Validation, E.S.S.; Formal analysis, N.V.S., E.S.S. and P.A.V.; Investigation, N.V.S., E.S.S. and P.A.V.; Resources, E.S.S. and P.A.V.; Data Curation, N.V.S. and P.A.V.; Writing—original draft preparation, N.V.S.; Writing—review and editing, N.V.S., E.S.S. and P.A.V.

Funding: This research received no external funding.

Acknowledgments: We gratefully acknowledge the continuous supervision and technical support of the geoelectrical stations of the VAN telemetric network by Basil Dimitropoulos, Spyros Tzigkos and George Lampithianakis.

Conflicts of Interest: The authors declare no conflict of interest.

Abbreviations

The following abbreviations are used in this manuscript:

ATH	Athens
EQ	Earthquake
ML(ATH)	Local EQ magnitude reported by the Institute of Geodynamics of the National Observatory of Athens
Mw	Moment magnitude
NTA	Natural time analysis
PAT	Patras SES measuring station
PIR	Pirgos SES measuring station
SES	Seismic Electric Signals
VAN	Varotsos Alexopoulos Nomikos

References

1. United States Geological Survey, Earthquake Hazards Program. M6.8-33km SW of Mouzaki, Greece. Available online: <https://earthquake.usgs.gov/earthquakes/eventpage/us1000hbb1/technical> (accessed on 10 May 2019)
2. Sarlis, N.V.; Skordas, E.S. Study in Natural Time of Geoelectric Field and Seismicity Changes Preceding the Mw6.8 Earthquake on 25 October 2018 in Greece. *Entropy* **2018**, *20*, 882. doi:10.3390/e20110882.
3. Varotsos, P. *The Physics of Seismic Electric Signals*; TERRAPUB: Tokyo, Japan, 2005.
4. Varotsos, P.A.; Sarlis, N.V.; Skordas, E.S. *Natural Time Analysis: The New View of Time. Precursory Seismic Electric Signals, Earthquakes and Other Complex Time-Series*; Springer: Berlin Heidelberg, Germany, 2011. doi:10.1007/978-3-642-16449-1.
5. Sarlis, N.V. Entropy in Natural Time and the Associated Complexity Measures. *Entropy* **2017**, *19*. doi:10.3390/e19040177.
6. Varotsos, P.; Lazaridou, M. Latest aspects of earthquake prediction in Greece based on Seismic Electric Signals. *Tectonophysics* **1991**, *188*, 321–347. doi:10.1016/0040-1951(91)90462-2.
7. Varotsos, P.; Alexopoulos, K.; Lazaridou, M. Latest aspects of earthquake prediction in Greece based on Seismic Electric Signals, II. *Tectonophysics* **1993**, *224*, 1 – 37. doi:10.1016/0040-1951(93)90055-O.
8. Sarlis, N.V. Statistical Significance of Earth's Electric and Magnetic Field Variations Preceding Earthquakes in Greece and Japan Revisited. *Entropy* **2018**, *20*, 561. doi:10.3390/e20080561.
9. Rundle, J.B.; Turcotte, D.L.; Donnellan, A.; Grant Ludwig, L.; Luginbuhl, M.; Gong, G. Nowcasting earthquakes. *Earth Space Sci.* **2016**, *3*, 480–486. doi:10.1002/2016EA000185.
10. Rundle, J.B.; Luginbuhl, M.; Giguere, A.; Turcotte, D.L. Natural Time, Nowcasting and the Physics of Earthquakes: Estimation of Seismic Risk to Global Megacities. *Pure Appl. Geophys.* **2018**, *175*, 647–660. doi:10.1007/s00024-017-1720-x.
11. Luginbuhl, M.; Rundle, J.B.; Hawkins, A.; Turcotte, D.L. Nowcasting Earthquakes: A Comparison of Induced Earthquakes in Oklahoma and at the Geysers, California. *Pure Appl. Geophys.* **2018**, *175*, 49–65. doi:10.1007/s00024-017-1678-8.
12. Luginbuhl, M.; Rundle, J.B.; Turcotte, D.L. Natural Time and Nowcasting Earthquakes: Are Large Global Earthquakes Temporally Clustered? *Pure Appl. Geophys.* **2018**, *175*, 661–670. doi:10.1007/s00024-018-1778-0.
13. Rundle, J.B.; Giguere, A.; Turcotte, D.L.; Crutchfield, J.P.; Donnellan, A. Global Seismic Nowcasting With Shannon Information Entropy. *Earth Space Sci.* **2019**, *6*, 191–197. doi:10.1029/2018EA000464.
14. Sarlis, N.V.; Skordas, E.S.; Varotsos, P.A. Geoelectric Field and Seismicity Changes Preceding the 2018 Mw6.8 Earthquake and the Subsequent Activity in Greece, 20 January 2019. arXiv:1901.06658v1 [physics.geo-ph]. Available online: <https://arxiv.org/abs/1901.06658v1> (accessed on 20 January 2019)
15. European Mediterranean Seismological Center. M5.4-GREECE- 2019-02-05 02:26:09 UTC. Available online: <https://www.emsc-csem.org/Earthquake/earthquake.php?id=742939> (accessed on 10 May 2019)
16. European Mediterranean Seismological Center. M5.3-GREECE-2019-03-30 10:46:18 UTC. Available online: <https://www.emsc-csem.org/Earthquake/earthquake.php?id=754693> (accessed on 10 May 2019)
17. Uyeda, S.; Al-Damegh, E.; Dologlou, E.; Nagao, T. Some relationship between VAN seismic electric signals (SES) and earthquake parameters. *Tectonophysics* **1999**, *304*, 41–55. doi:10.1016/S0040-1951(98)00301-1.

18. Sarlis, N.V.; Skordas, E.S.; Lazaridou, M.S.; Varotsos, P.A. Investigation of seismicity after the initiation of a Seismic Electric Signal activity until the main shock. *Proc. Jpn. Acad. Ser. B Phys. Biol. Sci.* **2008**, *84*, 331–343. doi:10.2183/pjab.84.331.
19. Varotsos, P.; Alexopoulos, K. Physical Properties of the variations of the electric field of the Earth preceding earthquakes, I. *Tectonophysics* **1984**, *110*, 73–98. doi:10.1016/0040-1951(84)90059-3.
20. Varotsos, P.; Alexopoulos, K. Physical Properties of the variations of the electric field of the Earth preceding earthquakes, II. *Tectonophysics* **1984**, *110*, 99–125. doi:10.1016/0040-1951(84)90060-X.
21. Lazaridou-Varotsos, M.S. *Earthquake Prediction by Seismic Electric Signals. The success of the VAN Method over thirty years*; Springer: Berlin Heidelberg, 2013.
22. Varotsos, P.; Alexopoulos, K. *Thermodynamics of Point Defects and Their Relation with Bulk Properties*; North Holland: Amsterdam, The Netherlands, 1986.
23. Varotsos, P. Point defect parameters in β -PbF₂ revisited. *Solid State Ionics* **2008**, *179*, 438–441. doi:10.1016/j.ssi.2008.02.055.
24. Varotsos, P.A.; Sarlis, N.V.; Skordas, E.S. Phenomena preceding major earthquakes interconnected through a physical model. *Ann. Geophys.* **2019**, *37*, 315–324. doi:10.5194/angeo-37-315-2019.
25. Sarlis, N.; Lazaridou, M.; Kapiris, P.; Varotsos, P. Numerical Model of the Selectivity Effect and $\Delta V/L$ criterion. *Geophys. Res. Lett.* **1999**, *26*, 3245–3248. doi:10.1029/1998GL005265.
26. Huang, Q.; Ikeya, M. Seismic electromagnetic signals (SEMS) explained by a simulation experiment using electromagnetic waves. *Phys. Earth Planet. Inter.* **1998**, *109*, 107–114. doi:10.1016/S0031-9201(98)00135-6.
27. Varotsos, P.; Sarlis, N.; Lazaridou, M.; Kapiris, P. Transmission of stress induced electric signals in dielectric media. *J. Appl. Phys.* **1998**, *83*, 60–70. doi:10.1063/1.366702.
28. Varotsos, P.; Sarlis, N.; Lazaridou, M. Transmission of stress induced electric signals in dielectric media. Part II. *Acta Geophys. Pol.* **2000**, *48*, 141–177.
29. Varotsos, P.; Sarlis, N.; Skordas, E. Transmission of stress induced electric signals in dielectric media. Part III. *Acta Geophys. Pol.* **2000**, *48*, 263–297.
30. Huang, Q. Controlled analogue experiments on propagation of seismic electromagnetic signals. *Chin. Sci. Bull.* **2005**, *50*, 1956–1961.
31. Huang, Q.; Lin, Y. Selectivity of seismic electric signal (SES) of the 2000 Izu earthquake swarm: a 3D FEM numerical simulation model. *Proc. Jpn Acad. Ser. B Phys. Biol. Sci.* **2010**, *86*, 257–264. doi:10.2183/pjab.86.257.
32. Varotsos, P.; Alexopoulos, K.; Nomicos, K. Seismic Electric Currents. *Pract. Athens Acad.* **1981**, *56*, 277–286.
33. Varotsos, P.; Alexopoulos, K.; Nomicos, K. Seven-hour precursors to earthquakes determined from telluric currents. *Pract. Athens Acad.* **1981**, *56*, 417–433.
34. Varotsos, P.A.; Sarlis, N.V.; Skordas, E.S. Detrended fluctuation analysis of the magnetic and electric field variations that precede rupture. *Chaos* **2009**, *19*, 023114. doi:10.1063/1.3130931.
35. Sarlis, N.V.; Skordas, E.S.; Varotsos, P.A. GEOELECTRIC Field and Seismicity Changes Preceding the 2018 Mw6.8 Earthquake and the Subsequent Activity in Greece, 17 April 2019. arXiv:1901.06658v2 [physics.geo-ph]. Available online <https://arxiv.org/abs/1901.06658v2>. (accessed on 17 April 2019)
36. Varotsos, P.A.; Sarlis, N.V.; Skordas, E.S.; Uyeda, S.; Kamogawa, M. Natural time analysis of critical phenomena. The case of Seismicity. *EPL* **2010**, *92*, 29002. doi:10.1209/0295-5075/92/29002.
37. Uyeda, S.; Kamogawa, M.; Tanaka, H. Analysis of electrical activity and seismicity in the natural time domain for the volcanic-seismic swarm activity in 2000 in the Izu Island region, Japan. *J. Geophys. Res.* **2009**, *114*. doi:10.1029/2007JB005332.
38. Varotsos, P.A.; Sarlis, N.V.; Skordas, E.S.; Christopoulos, S.R.G.; Lazaridou-Varotsos, M.S. Identifying the occurrence time of an impending mainshock: A very recent case. *Earthq. Sci.* **2015**, *28*, 215–222. doi:10.1007/s11589-015-0122-3.
39. Varotsos, P.A.; Sarlis, N.V.; Skordas, E.S. Identifying the occurrence time of an impending major earthquake: a review. *Earthq. Sci.* **2017**, *30*, 209–218. doi:10.1007/s11589-017-0182-7.
40. Varotsos, P.A.; Sarlis, N.V.; Skordas, E.S. Spatio-Temporal complexity aspects on the interrelation between Seismic Electric Signals and Seismicity. *Pract. Athens Acad.* **2001**, *76*, 294–321.
41. Varotsos, P.A.; Sarlis, N.V.; Skordas, E.S. Long-range correlations in the electric signals that precede rupture. *Phys. Rev. E* **2002**, *66*, 011902. doi:10.1103/physreve.66.011902.

42. Varotsos, P.A.; Sarlis, N.V.; Skordas, E.S. Seismic Electric Signals and Seismicity: On a tentative interrelation between their spectral content. *Acta Geophys. Pol.* **2002**, *50*, 337–354.
43. Tanaka, H.K.; Varotsos, P.A.; Sarlis, N.V.; Skordas, E.S. A plausible universal behaviour of earthquakes in the natural time-domain. *Proc. Jpn. Acad. Ser. B Phys. Biol. Sci.* **2004**, *80*, 283–289. doi:10.2183/pjab.80.283.
44. Varotsos, P.; Sarlis, N.; Skordas, E. On the Motivation and Foundation of Natural Time Analysis: Useful Remarks. *Acta Geophys.* **2016**, *64*, 841 – 852. doi:10.1515/acgeo-2016-0031.
45. Varotsos, P.A.; Sarlis, N.V.; Skordas, E.S. Long-range correlations in the electric signals the precede rupture: Further investigations. *Phys. Rev. E* **2003**, *67*, 021109. doi:10.1103/PhysRevE.67.021109.
46. Varotsos, P.A.; Sarlis, N.V.; Skordas, E.S. Attempt to distinguish electric signals of a dichotomous nature. *Phys. Rev. E* **2003**, *68*, 031106. doi:10.1103/PhysRevE.68.031106.
47. Varotsos, P.; Sarlis, N.V.; Skordas, E.S.; Uyeda, S.; Kamogawa, M. Natural time analysis of critical phenomena. *Proc. Natl. Acad. Sci. USA* **2011**, *108*, 11361–11364. doi:10.1073/pnas.1108138108.
48. Varotsos, P.A.; Sarlis, N.V.; Skordas, E.S.; Lazaridou, M.S. Entropy in Natural Time Domain. *Phys. Rev. E* **2004**, *70*, 011106. doi:10.1103/physreve.70.011106.
49. Varotsos, P.A.; Sarlis, N.V.; Tanaka, H.K.; Skordas, E.S. Some properties of the entropy in the natural time. *Phys. Rev. E* **2005**, *71*, 032102. doi:10.1103/physreve.71.032102.
50. Lesche, B. Instabilities of Renyi entropies. *J. Stat. Phys.* **1982**, *27*, 419. doi:10.1007/BF01008947.
51. Lesche, B. Renyi entropies and observables. *Phys. Rev. E* **2004**, *70*, 017102. doi:10.1103/PhysRevE.70.017102.



© 2019 by the authors. Licensee MDPI, Basel, Switzerland. This article is an open access article distributed under the terms and conditions of the Creative Commons Attribution (CC BY) license (<http://creativecommons.org/licenses/by/4.0/>).